Clays and Clay Minerals, Vol. 57, No. 6, 771–778, 2009.

CRYSTALLOGRAPHIC SITE DISTRIBUTION AND REDOX ACTIVITY OF Fe IN NONTRONITES DETERMINED BY OPTICAL SPECTROSCOPY

ROSE B. MEROLA AND MOLLY M. MCGUIRE*

Department of Chemistry, Bucknell University, Lewisburg, PA 17837, USA

Abstract—Optical absorption spectroscopy has the potential to uncover many characteristics of Fe-bearing, redox-active smectites that have heretofore been hidden. The purpose of this study was to exploit this technique to reveal the temperature dependence of the spectra and to characterize the behavior of octahedral and tetrahedral Fe(III) under various stages of reduction. The Uley nontronites, NAu-1 and NAu-2, were compared using optical spectroscopy, which probed the crystallographic-site distribution of Fe in the clay structures as well as the resulting differences in the reduction process in the two minerals. All of the major differences in the spectra of the two minerals in the wavelength range 450−950 nm are due to the presence of a significant amount of tetrahedral Fe(III) in NAu-2. *In situ* observation of the optical spectra of NAu-1 suspensions as a function of the degree of reduction reveals a steady increase in the dominant intervalence charge transfer (IVCT) band and the resulting blue-green color as the Fe(II) content of the octahedral sheet increases. Although the spectrum of NAu-2 at ~50% reduction looks nearly identical to the spectrum of NAu-1 at a similar state of reduction, the spectra corresponding to the initial stages of reduction are quite different. Stepwise reduction of NAu-2 causes a rapid decrease in the absorbance features due to crystal-field transitions of tetrahedral Fe(III) before the IVCT band appears, suggesting that tetrahedral Fe(III) is preferentially reduced before the octahedral Fe(III). The intensity of the absorbance features due to tetrahedral Fe(III) also exhibit an inverse temperature dependence, suggesting that they are enhanced due to exchange-coupling with Fe(III) ions in neighboring sites. Spectra of NAu-1 at liquid nitrogen temperature, therefore, allowed the identification of a small amount of tetrahedral Fe(III) in NAu-1 that had not been noted previously.

Key Words—NAu-1, NAu-2, Nontronites, Optical Spectra, Reduction, Tetrahedral Fe(III).

INTRODUCTION

Clay minerals are an important source of redox-active Fe in soils and sediments. Structural Fe(III) can be reduced by microorganisms, resulting in changes to many properties of the mineral, including surface-charge density, swelling, and Brønsted basicity of surface sites (Kostka *et al*., 1999; Stucki *et al*., 2002). The reduced forms of several Fe-bearing clay minerals have also been shown to effect the chemical transformation of common groundwater contaminants such as pesticides (Boparai *et al*., 2006; Ribeiro *et al*., 2004; Sorensen *et al*., 2004; Tor *et al.*, 2000; Xu *et al*., 2001), nitroaromatic compounds (Elsner *et al*., 2004; Hofstetter *et al*., 2003, 2006; Schultz and Grundl, 2000; Yan and Bailey, 2001; Neumann *et al*., 2008), and organohalides (Cervini-Silva *et al*., 2000, 2001, 2003; Elsner *et al*., 2004; Jung and Batchelor, 2007; Kriegman-King and Reinhard, 1992; Nzengung *et al.*, 2001).

The Uley nontronites, NAu-1 and NAu-2, from the Source Clays Repository of The Clay Minerals Society (based at Purdue University, West Lafayette, Indiana) have recently become popular model systems for laboratory investigations of the redox activity of structural Fe in clay minerals (Jaisi *et al*., 2005, 2007; Kim *et al.*, 2005; Li *et al.*, 2004; O'Reilly *et al*., 2005; Zhang *et al*., 2007). NAu-1 and NAu-2 have the formulae

$$M^{+}_{1.02}[Si_{6.98}Al_{0.95}Fe_{0.07}][Al_{0.36}Fe_{3.61}Mg_{0.04}]O_{20}(OH)_4$$

and

$$M^{+}_{0.72}[Si_{7.55}Al_{0.16}Fe_{0.29}][Al_{0.34}Fe_{3.54}Mg_{0.05}]O_{20}(OH)_4,$$

respectively (Gates *et al*., 2002). As indicated by their formulae, the two clays are thought to differ significantly in terms of the distribution of Fe within the mineral. Elemental analyses revealed that NAu-2 has an insufficient amount of Al^{3+} to fill available tetrahedral sites, suggesting that a significant amount of Fe(III) must be present in the tetrahedral sheets (Keeling *et al.*, 2000). Gates *et al.* (2002) performed a comprehensive comparison of a series of nontronites and ferruginous smectites employing a range of techniques including near-infrared (NIR) spectroscopy, X-ray near-edge and X-ray fine-structure absorption spectroscopies, and X-ray diffraction (XRD), and concluded that up to ~10% of Fe(III) in NAu-2 is contained within the tetrahedral sheet. A recent Mössbauer spectroscopy study also concluded that NAu-2 must contain tetrahedral Fe(III) (Jaisi *et al.*, 2005).

As is the case with many minerals, the presence of Fe, and in particular the oxidation-state distribution of

* E-mail address of corresponding author:
mmcguire@bucknell.edu
DOI: 10.1346/CCMN.2009.0570609

Fe across the available structural sites, determines the color of nontronites. Consequently, visible spectroscopy can be used as a tool to investigate the electronic structure and redox processes in Fe-bearing clay minerals. Several compilations of the optical spectra of Fe-bearing clay minerals have appeared in the literature (Karickhoff and Bailey, 1973; Sherman and Vergo, 1988), while other studies have used optical spectra to follow the reduction process in Fe-bearing clays (Anderson and Stucki, 1979; Lear and Stucki, 1987) or the interactions of Fe^{2+}(aq) with nontronite edge sites (Merola *et al.*, 2007).

Despite the increasing use of the Uley nontronites as model systems for redox studies and the demonstrated utility of optical spectroscopy for understanding redox transformations, the optical spectra of these minerals have not yet been analyzed in detail. In the present study, optical spectra of the Uley nontronites in their untreated states and as a function of the degree of reduction of the structural Fe(III) were examined. Comparison of the two minerals provides information not only about the differences in their structure and their redox activity, but offers insight into the influence of Fe(III) site occupancy on the redox properties of Fe-bearing clay minerals in general.

MATERIALS AND METHODS

Purification of the clay mineral

NAu-1 and NAu-2, both nontronites from the Uley Graphite Mine in Australia, were purchased from the Source Clays Repository of The Clay Minerals Society. A wet sedimentation process (Vaniman, 2001) was used to isolate the 0.35−2 μm size fraction of the mineral. Once the appropriate size fraction was collected, the clays were acid washed with 0.1 M acetic acid (Baker, Phillipsburg, New Jersey, USA) in order to eliminate acid-soluble mineral phases such as carbonates, and then rinsed three times with 18 MΩ-cm deionized water. Infrared spectroscopy was used to verify the purity of the resulting samples (data not shown). As previously noted (Keeling *et al.*, 2000), evidence of small amounts of kaolinite was found in the IR spectra of NAu-1. Finally, Na^+-saturated samples were produced by washing the clays with 0.1 M NaCl (Fisher, Fair Lawn, New Jersey, USA) followed by three washes with 18 MΩ-cm deionized water.

Reduction of the clay minerals

The clays were reduced in a stepwise fashion in order to investigate the evolution of the optical spectra as a function of the degree of reduction. All solutions and suspensions were prepared within an anaerobic glovebox under an atmosphere of 95:5 N_2:H_2. Approximately 0.5 g of clay was suspended in 20 mL of an N_2-sparged sodium citrate-bicarbonate buffer consisting of one part 0.3 M sodium citrate, $Na_3C_6H_5O_7{\cdot}2H_2O$ (Baker), and eight parts of 1 M sodium bicarbonate, $NaHCO_3$ (Spectrum, Gardena, California, USA). Approximately 0.002 g of sodium dithionite, $Na_2S_2O_4$ (Matheson, Norwood, Ohio, USA), was added as the reducing agent. The clay suspension was heated to 70ºC for at least 15 min, and then allowed to cool to room temperature before a diffuse reflectance spectrum was obtained (see below). Another aliquot of sodium dithionite was added and another spectrum was acquired. This process was repeated to produce a series of snapshots of the reduction process. Although the actual degree of reduction as a percent of total Fe is not known, the series of spectra for each mineral correspond to increasing degrees of reduction.

Diffuse reflectance spectroscopy

Spectra were acquired using a USB2000 UV-vis spectrometer coupled to a tungsten halogen light source and reflectance fiber optic probe, all from Ocean Optics (Dunedin, Florida, USA). The reflectance probe consisted of a bundle of six 400-μm diameter illumination fibers around one read fiber. The entire experimental apparatus was contained in the anaerobic glovebox. Spectra of the colloidal samples were acquired by immersing the fiber optic probe directly into the suspension. Although variation in particle size and/or density would be expected to result in changes in the reflection spectra, each series of spectra corresponding to increasing degrees of reduction were obtained from the same suspension, thus allowing direct comparison of the spectra within a series. Data were acquired in the range 450−950 nm with an integration time of 200−800 ms. Final spectra were the result of ~20 averaged scans. Values of percent reflectance were calculated relative to a diffuse reflectance standard (WS-1, Ocean Optics), which provided a Lambertian reference surface with >98% reflectivity over the examined wavelength range. Raw reflectance data were transformed by the Kubelka-Munk (1931) remission function. Assuming that the scattering coefficient is approximately constant over the wavelength range investigated, the Kubelka-Munk spectra are equivalent to absorbance spectra and are referred to as such throughout this paper. All spectra were smoothed by the Savitzky-Golay algorithm using the software package *PeakFit* (Systat, San Jose, California, USA). Calculation of the second derivative of spectra for the purposes of determining peak intensities was also performed by the Savitsky-Golay method using *PeakFit*.

Low-temperature studies

For the spectra of clay at low temperatures, self-supported films of the clay were produced by allowing a dense suspension of the mineral to air-dry on a glass substrate. Once dry, the clay film was scraped from the glass in large flakes. The dried clay films were placed on a copper stand that was immersed in a dewar containing liquid nitrogen. Although the clay itself was not in

https://doi.org/10.1346/CCMN.2009.0570609 Published online by Cambridge University Press

contact with the liquid nitrogen, the copper acted as an efficient heat transfer medium and the temperature of the clay was close to that of the liquid nitrogen. Spectra were then obtained by placing the reflectance probe directly over the clay sample.

RESULTS AND DISCUSSION

Absorption spectra

The yellow-green NAu-1 and the brown NAu-2 have very different absorbance features in the 450–950 nm region of the spectrum (Figure 1). The only observable feature in the spectrum of NAu-1 is the tail end of an absorption band that resides out of the experimental wavelength range toward the UV region of the spectrum. This feature is due to the $^6A_{1g} \rightarrow {}^4T_2(^4D)$ crystal-field transition of octahedral Fe(III), which appears near 380 nm (26,000 cm^{-1}) in nontronites (Sherman and Vergo, 1988). In contrast, NAu-2 has a broad, pronounced absorption plateau that begins at ~570 nm and extends toward the shorter wavelengths. One possible contribution to this region of the spectrum is the pair excitation of exchange-coupled Fe(III) ions that reside in adjacent sites within the octahedral sheet. Double excitations of this type ($2[^6A_{1g}] \rightarrow 2[^4T_{1g}]$) have been noted at ~450 nm in the spectra of other nontronites (Sherman and Vergo, 1988). The absence of this feature in the spectrum of NAu-1, presumably due to a lack of exchange-coupled Fe(III) ions in adjacent sites, may be explained by the difference in the distribution of Fe(III) across the available sites in the octahedral sheets of the two minerals. In NAu-2, Fe(III) is found in both *cis*- and *trans*-dihydroxyl sites in the octahedral sheet. In contrast, Fe(III) occupies only the *cis*-dihydroxyl sites in NAu-1 (Jaisi *et al*., 2005). Another possible assignment for the 450 nm band in the spectra of nontronites is the $^6A_1 \rightarrow {}^2T_{1g}$ and $^6A_1 \rightarrow {}^2A_{2g}$ transitions of octahedral Fe(III) (Sherman and Vergo, 1988).

The breadth of the absorption features observed between 450 and 570 nm in the spectrum of NAu-2 suggests that it is made up of several broad, overlapping bands, and clearly another absorption band must be present on the long-wavelength side of the pair transition. Molecular orbital calculations (Sherman, 1985) of Fe oxide minerals have shown that the $^6A_1 \rightarrow {}^4T_2(^4G)$ of tetrahedrally coordinated Fe(III) should appear at ~525 nm. Although Gates *et al.* (2002) found that tetrahedral Fe accounts for ~10% of the total Fe in NAu-2, crystal-field transitions of Fe(III) in the non-centrosymmetric tetrahedral sites are Laporte-allowed and, therefore, are more intense than those of the octahedral species (Burns, 1993). Consequently, the seemingly small quantities of tetrahedral Fe(III) may have a very significant effect on the spectra.

An additional intense absorption band is observed in the spectrum of NAu-2 at ~650 nm, coinciding well with the calculated energy of the $^6A_1 \rightarrow {}^4T_1(^4G)$ crystal field transition of Fe(III) in tetrahedral coordination (Sherman, 1985). Sherman and Vergo (1988) assigned absorption bands at similar energies in the spectra of several nontronites to the $^6A_{1g} \rightarrow {}^4T_{2g}$ transition of octahedral Fe(III). As mentioned above, the significantly greater intensity of transitions due to tetrahedrally coordinated Fe(III) as compared to octahedral Fe(III) provides a reasonable justification for assuming that this strong absorption band is mostly due to the tetrahedral species. In addition, the absence of these features in the spectra of NAu-1 is consistent with the very small tetrahedral Fe(III) content of NAu-1 (Gates *et al.*, 2002).

Reduction process

Despite the very distinct optical spectra of the two nontronites in their untreated states, the chemically

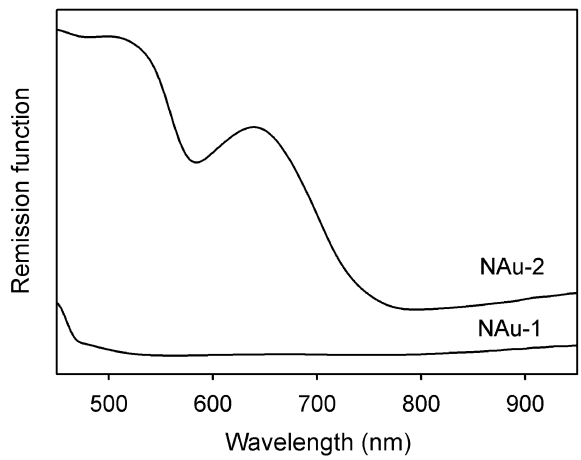

Figure 1. Relative absorbance of NAu-1 and NAu-2 suspensions as given by the Kubelka-Munk remission function. Plots have been offset for clarity.

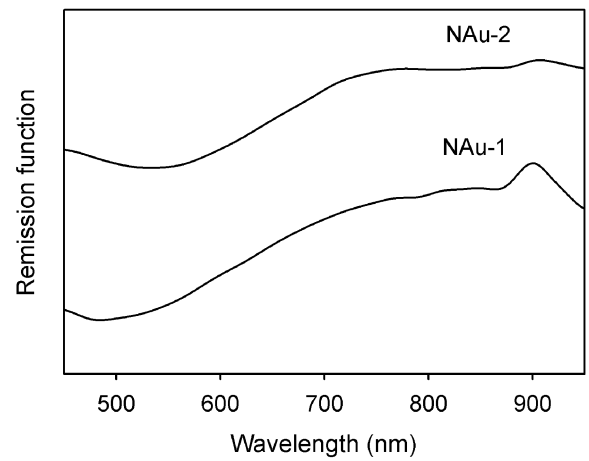

Figure 2. Relative absorbance of chemically reduced NAu-1 and NAu-2 films as given by the Kubelka-Munk remission function. Plots have been offset for clarity.

https://doi.org/10.1346/CCMN.2009.0570609 Published online by Cambridge University Press

reduced forms of the minerals exhibit nearly identical spectra (Figure 2). Treatment with sodium dithionite turned suspensions of both nontronites a brilliant blue-green. The color change is the result of an absorbance feature with a maximum at ~750 nm, which extends toward higher wavelengths. This absorption feature can be assigned to the strong intervalence charge transfer (IVCT) transitions that have been well characterized in reduced nontronites (Lear and Stucki, 1987) and other mixed valency, Fe-bearing clay minerals (Burns, 1981; Smith and Strens, 1976). Such transitions occur when Fe(III) and Fe(II) occupy adjacent, edge-sharing octahedral sites in the nontronite structure and absorption causes transfer of charge from the Fe(II) to the Fe(III). In addition, a much weaker feature is seen near 900 nm in the spectrum of NAu-1, and to a lesser extent, in the spectrum of NAu-2. This absorption band can be assigned to the presence of octahedrally coordinated Fe(II) (Sherman and Vergo, 1988). Crystal-field transitions of tetrahedral Fe(II), which might also be expected to appear in the spectrum of NAu-2, are found in the NIR region of the spectrum (Rossman, 1988) beyond the experimental range of these studies. The IVCT transitions between the tetrahedral sheet and octahedral sheet are not observed either. The absence of such features is not surprising as IVCT transitions have only been observed between ions in edge- or face-sharing polyhedra (Burns, 1981; Smith and Strens, 1976), while the tetrahedra and octahedra of smectites share corners.

The similarity of the spectra of the reduced minerals despite the dissimilarity of those of the untreated minerals suggests that examination of the reduction process in incremental steps for each of the minerals should provide clues as to the difference in their reactivities and reduction pathways. Spectra of a suspension of NAu-1 as it was incrementally reduced (Figure 3) are arranged in order of increasing degrees of reduction from bottom to top. As reduction proceeds, the major change in the spectra is the increasing intensity of the IVCT feature at ~750 nm, indicating that Fe(III) within the octahedral sheet is being reduced. If reduction continued, the intensity of this feature should eventually decrease as most of the Fe(II) created by the reduction process will not be located adjacent to Fe(III) in neighboring sites, as reported by Komadel et al. (1990) for other nontronites. In the case illustrated here, the continuing increase in intensity of the IVCT feature indicates that the reduction of the mineral was not complete.

The stepwise reduction of NAu-2 (Figure 4) reveals several details of the reactivity of this mineral towards reduction. In particular, both absorption features assigned to the $^6A_1 \rightarrow {}^4T_2(^4G)$ and $^6A_1 \rightarrow {}^4T_1(^4G)$ crystal-field transitions of tetrahedral Fe(III) at 525 and 650 nm, respectively, lose intensity before a substantial increase in intensity is seen in the IVCT transition at ~750 nm. In addition, a comparison of Figures 3 and 4 reveals that the spectra of NAu-2 (Figure 4) exhibit a lower IVCT intensity than the spectra of NAu-1 (Figure 3) at any given level of reduction.

To examine these trends in peak intensity more quantitatively, the second-derivative method was employed (Scheinost *et al.*, 1998). An example of a second-derivative spectrum for a partially reduced sample of NAu-2 is shown in Figure 5. The peaks at 650 and 750 nm appear as minima in the second-derivative spectra, and the amplitudes of these features were measured as indicated in Figure 5.

The peak amplitudes changed as a function of the amount of reductant added to each of the suspensions (Figure 6) and the major trends in the spectra from conventional spectra (Figures 3 and 4) are readily apparent in the amplitudes obtained from the second derivative plots (Figure 6). The intensity of the 650 nm band in NAu-2 decreased very quickly through the early stages of reduction, while the intensity of the IVCT band

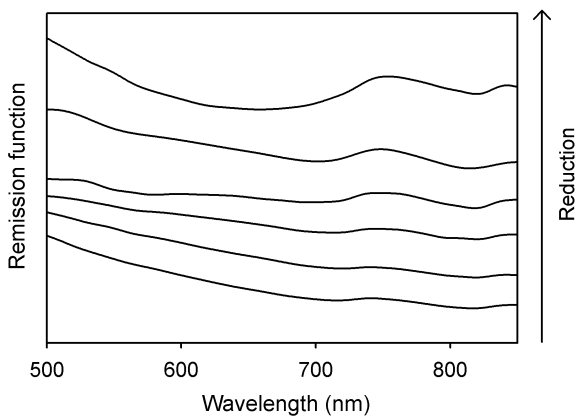

Figure 3. Relative absorbance of an NAu-1 suspension at various stages of reduction as given by the Kubelka-Munk remission function. The extent of reduction increases stepwise in the spectra from the bottom of the figure to the top.

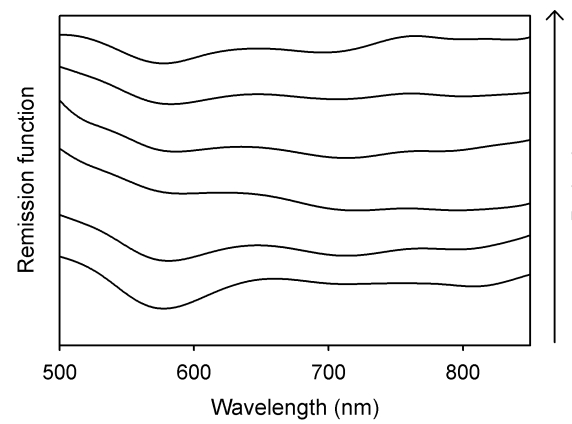

Figure 4. Relative absorbance of an NAu-2 suspension at various stages of reduction as given by the Kubelka-Munk remission function. The extent of reduction increases stepwise in the spectra from the bottom of the figure to the top.

https://doi.org/10.1346/CCMN.2009.0570609 Published online by Cambridge University Press

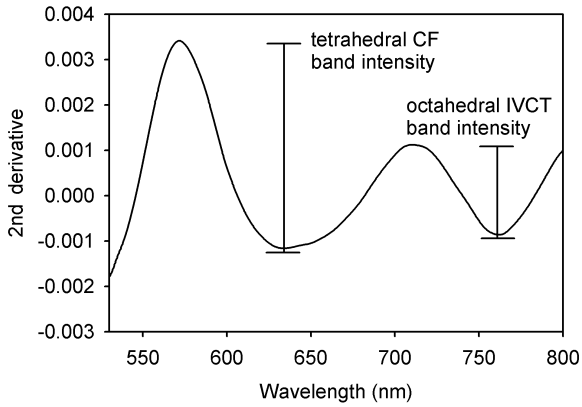

Figure 5. The second derivative of the remission function for a sample of partially reduced NAu-2. The minima in the spectrum correspond to the peak positions of the observed absorption features. The bars on the figure indicate the measured amplitudes of the tetrahedral crystal field (CF) transition and the octahedral IVCT transition, respectively.

at 750 nm remains relatively constant before finally beginning to increase after addition of 12 mg of sodium dithionite. In contrast, the feature at 750 nm in the NAu-1 spectra increases fairly steadily as reduction proceeds.

Because the reduction of Fe(III) in the octahedral sheet would result in the simultaneous appearance of a strong absorption feature due to IVCT transitions with neighboring Fe(III) ions, the disappearance of the absorption bands at 525 nm and 650 nm at the early stages of reduction of NAu-2 – before any significant increase in the IVCT band – is further evidence that these bands must be due to tetrahedral Fe(III) and also suggests that tetrahedral Fe(III) is preferentially reduced first in NAu-2. Findings from a recent Mössbauer study (Jaisi *et al*., 2005) of the microbiological reduction of NAu-2 concluded that Fe(III) in tetrahedral sites, as well as *trans*-dihydroxyl octahedral sites, was more easily reduced than the more abundant Fe(III) in *cis*-dihdroxyl octahedral sites. The results of the present *in situ* study, which allowed for the observation of incremental steps of reduction, suggest that, in fact, tetrahedral Fe(III) is reduced before octahedral Fe(III) is reduced to any appreciable extent.

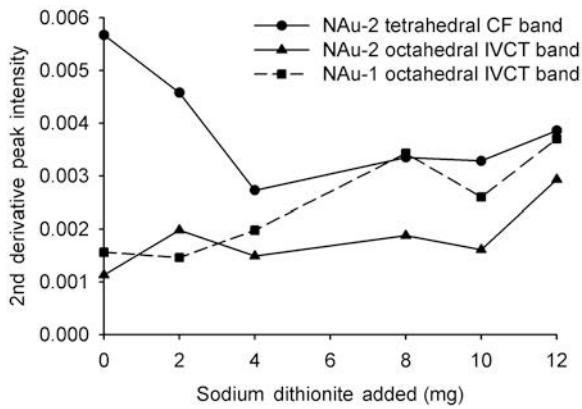

Figure 6. Amplitude of the peaks associated with the crystal field transition of tetrahedral Fe(III) in NAu-2 (circles) and the IVCT bands of octahedral Fe in NAu-2 (triangles) and NAu-1 (squares) as a function of the amount of sodium dithionite added. Peak amplitudes were determined as illustrated in Figure 5.

An important point to note is that the IVCT band resulting from the reduction of octahedral Fe(III) should exhibit maximum intensity when ~50% of the octahedral Fe(III) has been reduced (Lear *et al.*, 1987). The lack of intensity in the IVCT band observed through the first few reduction steps in this study could, in principle, indicate that >50% of the octahedral Fe(III) was reduced immediately and the subsequent reduction steps, therefore, do not result in an increase in the IVCT band. A simple stoichiometric analysis, however, indicates that this scenario is not possible. Assuming the formula, $M^{+}_{0.72}[Si_{7.55}Al_{0.16}Fe_{0.29}][Al_{0.34}Fe_{3.54}Mg_{0.05}]O_{20}(OH)_4$, for NAu-2, the mineral contains 25% Fe by weight. Therefore, the 0.5 g of clay mineral used in the stepwise reduction contains ~0.002 moles of Fe. Assuming that the reduction reaction goes to completion, each addition of sodium dithionite (0.002 g or 1×10^{-5} moles) is capable of increasing the total Fe(II) content in NAu-2 by at most ~1%. Consequently, the spectra presented in Figure 4 must all correspond to points before the maximum in the IVCT transition is reached, confirming that the low intensity of the IVCT band is the result of small rather than large quantities of octahedral Fe(II). This result, coupled with the observed disappearance of the bands due to tetrahedral species at 525 and 650 nm before the appearance of the IVCT band at 750 nm, confirms that tetrahedral Fe(III) is indeed reduced before octahedral Fe(III).

Low-temperature studies

The temperature dependence of the spectrum of NAu-2 reveals additional information about the nature of the observed transitions. Comparison of the spectra of a film of NAu-2 at room temperature and a film at liquid nitrogen temperature (Figure 7) revealed that both major absorption regions are clearly inversely dependent on temperature and increase in intensity at lower temperatures. The 525 nm absorption feature was also shifted slightly toward 500 nm.

The inverse temperature dependence of the absorption features in NAu-2 is unusual for crystal-field transitions; the behavior is more often associated with charge-transfer transitions (Smith and Strens, 1976). However, crystal-field transitions of ions in exchange-coupled pairs have been shown to exhibit an increase in intensity upon cooling (Taran *et al*., 1996). In the present case, the inverse temperature dependence, which causes NAu-2 to turn a bright green color at low temperatures, has been noted previously (Wu *et al.*, 2004), but the exact mechanism has not been identified. The crystal-

https://doi.org/10.1346/CCMN.2009.0570609 Published online by Cambridge University Press

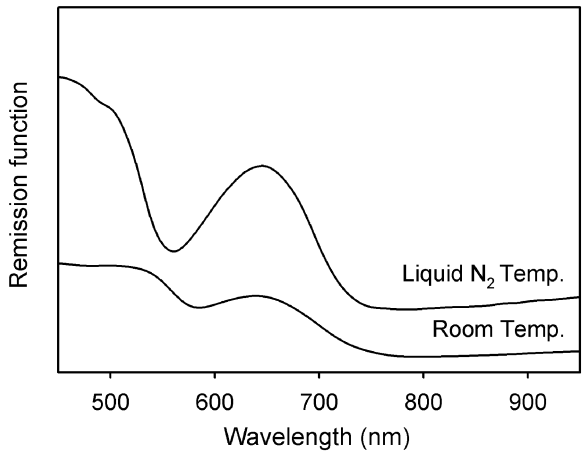

Figure 7. Relative absorbance of NAu-2 films at room and liquid nitrogen temperatures as given by the Kubelka-Munk remission function. Plots have been offset for clarity.

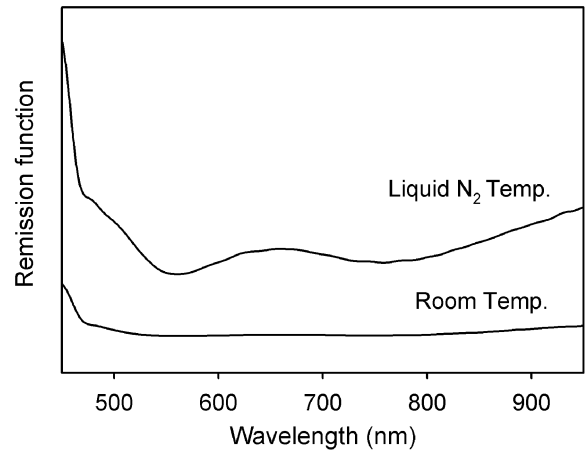

Figure 8. Relative absorbance of NAu-1 films at room and liquid nitrogen temperatures as given by the Kubelka-Munk remission function. Plots have been offset for clarity.

field transitions of tetrahedral Fe(III) observed in NAu-2 at 650 and 525 nm are proposed to be due to ions which are exchange-coupled to neighboring Fe(III) ions. The assignment provides an additional explanation for the high intensity of these features as transitions of Fe(III) in exchange-coupled pairs are often much more intense than the corresponding transitions of isolated Fe(III) ions (Rossman, 1988). A complete description of exchange coupling in these minerals is beyond the scope of the present study, but further investigation into this phenomenon and the implications for understanding the electronic structure of tetrahedral Fe(III)-containing nontronites is warranted.

For the purposes of the present study, the intensification of the tetrahedral Fe(III) transitions at low temperatures was used to probe NAu-1 for the possible presence of tetrahedral Fe(III) at very low concentrations. The absorption bands at 525 and 650 nm due to tetrahedral Fe(III), while absent from the room-temperature spectra, are both present in the spectrum of NAu-1 when the clay is cooled to liquid nitrogen temperature (Figure 8), but the bands are much weaker than in the spectrum of NAu-2 at the same low temperature. Because these features are not observed at room temperature and are only barely visible at low temperatures, NAu-1 must contain only a small amount of tetrahedral Fe(III). The fact that Mössbauer spectroscopy studies of NAu-1 failed to identify the presence of tetrahedral Fe(III) (Jaisi *et al.*, 2005) is not surprising because the interpretation of Mössbauer spectra with regard to tetrahedral Fe(III) is not always straightforward, as highlighted by the disagreements in the literature (Cardile, 1989; Luca and Cardile, 1989).

CONCLUSIONS

The results presented provide the first reported explanation for the temperature-dependent color changes of Fe-bearing clays. If the temperature dependence of the absorption bands in NAu-1 and NAu-2 are common to other smectites with tetrahedral Fe(III), low-temperature optical spectroscopy may provide a universal method to identify the presence of tetrahedral Fe(III) at low concentrations. Further investigation into the nature of exchange-coupling in nontronites and other Fe-bearing smectites is necessary to fully elucidate the applicability of this approach to the identification of tetrahedral Fe(III). In particular, the question remains of whether the presence of Fe(III) ions in adjacent crystallographic sites in the octahedral sheet is sufficient for the temperature-dependent enhancement of the tetrahedral transitions, or whether the specific distribution of Fe(III) within the octahedral sheet plays some role in the pair interactions.

The findings presented here also have implications for understanding differences in the redox activity of Fe-bearing clay minerals in geochemical cycles and the reduction of environmentally relevant chemical species. Tetrahedrally coordinated Fe in smectites is often ignored in laboratory studies, presumably due to the difficulty in identifying it. As suggested by its susceptibility to reduction in these studies, tetrahedral Fe may in fact play a major role in the Fe redox chemistry of clay minerals. The routine use of low-temperature optical spectroscopy, which allows detection of tetrahedral Fe at concentrations below the detection limits of other techniques, will allow for further investigations into the site-specific reactivity of Fe in clay minerals.

REFERENCES

Anderson, W.L. and Stucki, J.W. (1979) Effect of structural Fe^{2+} on visible absorption spectra of nontronite suspensions. Pp. 75–83 in: *Proceedings of the VI International Clay Conference* (M.M. Mortland and V.C. Farmer, editors). Elsevier, Amsterdam.

https://doi.org/10.1346/CCMN.2009.0570609 Published online by Cambridge University Press

Boparai, H.K., Shea, P.J., Comfort, S.D., and Snow, D.D. (2006) Dechlorinating chloroacetanilide herbicides by dithionite-treated aquifer sediment and surface soil. *Environmental Science & Technology*, **40**, 3043–3049.

Burns, R.G. (1981) Intervalence transitions in mixed-valence minerals of iron and titanium. *Annual Reviews in Earth and Planetary Science*, **9**, 345–383.

Burns, R.G. (1993) *Mineralogical Applications of Crystal Field Theory*. Cambridge University Press, Cambridge, UK.

Cardile, C.M. (1989) Tetrahedral iron in smectite: a critical comment. *Clays and Clay Minerals*, **37**, 185–188.

Cervini-Silva, J., Wu, J., Larson, R.A., and Stucki, J.W. (2000) Transformation of chloropicrin in the presence of iron-bearing clay minerals. *Environmental Science & Technology*, **34**, 915–917.

Cervini-Silva, J., Larson, R.A., Wu, J., and Stucki, J.W. (2001) Transformation of chlorinated aliphatic compounds by ferruginous smectite. *Environmental Science & Technology*, **35**, 805–809.

Cervini-Silva, J., Kostka, J.E., Larson, R.A., Stucki, J.W., and Wu, J. (2003) Dehydrochlorination of 1,1,1-trichloroethane and pentachloroethane by microbially reduced ferruginous smectite. *Environmental Toxicology and Chemistry*, **22**, 1046–1050.

Elsner, M., Schwarzenbach, R.P., and Haderlein, S.B. (2004) Reactivity of Fe(II)-bearing minerals toward reductive transformation of organic contaminants. *Environmental Science & Technology*, **38**, 799–807.

Gates, W.P., Slade, P.G., Manceau, A., and Lanson, B. (2002) Site occupancies by iron in nontronites. *Clays and Clay Minerals*, **50**, 223–239.

Hofstetter, T.B., Schwarzenbach, R.P., and Haderlein, S.B. (2003) Reactivity of Fe(II) species associated with clay minerals. *Environmental Science & Technology*, **37**, 519–528.

Hofstetter, T.B., Neumann, A., and Schwarzenbach, R.P. (2006) Reduction of nitroaromoatic compounds by Fe(II) species associated with iron-rich smectites. *Environmental Science & Technology*, **40**, 235–242.

Jaisi, D.P., Kukkadapu, R.K., Eberl, D.D., and Dong, H. (2005) Control of Fe(III) site occupancy on the rate and extent of microbial reduction of Fe(III) in nontronite. *Geochimica et Cosmochimica Acta*, **69**, 5429–5440.

Jaisi, D.P., Dong, H., and Liu, C. (2007) Kinetic analysis of microbial reduction of Fe(III) in nontronite. *Environmental Science & Technology*, **41**, 2437–2444.

Jung, B. and Batchelor, B. (2007) Influence of iron-bearing phyllosilicates on the dechlorination kinetics of 1,1,1-trichloroethane in Fe(II)/cement slurries. *Chemosphere*, **68**, 1254–1261.

Karickhoff, S.W. and Bailey, G.W. (1973) Optical absorption spectra of clay minerals. *Clays and Clay Minerals*, **21**, 59–70.

Keeling, J.L., Raven, M.D., and Gates, W.P. (2000) Geology and characterization of two hydrothermal nontronites from weathered metamorphic rocks at the Uley graphite mine, South Australia. *Clays and Clay Minerals*, **48**, 537–548.

Kim, J., Furukawa, Y., Dong, H., and Newell, S.W. (2005) The effect of microbial Fe(III) reduction on smectite flocculation. *Clays and Clay Minerals*, **53**, 572–579.

Komadel, P., Lear, P.R., and Stucki, J.W. (1990) Reduction and reoxidation of nontronite: Extent of reduction and reaction rates. *Clays and Clay Minerals*, **38,** 203-208.

Kostka, J.E., Wu, J., Nealson, K.H., and Stucki, J.W. (1999) The impact of structural Fe(III) reduction by bacteria on the surface chemistry of smectite clay minerals. *Geochimica et Cosmochimica Acta*, **63**, 3705–3713.

Kriegman-King, M.R. and Reinhard, M. (1992) Transformation of carbon tetrachloride in the presence of sulfide, biotite and vermiculite. *Environmental Science & Technology*, **26**, 2198–2206.

Kubelka, P. and Munk, F. (1931) Ein beitrig zur optik der Farbanstriche. *Zeitschrift fur technische Physik*, **12**, 593–620.

Lear, P.R. and Stucki, J.W. (1987) Intervalence electron transfer and magnetic exchange in reduced nontronite. *Clays and Clay Minerals*, **35**, 373–378.

Li, Y., Vali, H., Sears, S.K., Yang, J., Deng, B., and Zhang, C.L. (2004) Iron reduction and alteration of nontronite NAu-2 by a sulfate-reducing bacterium. *Geochimica et Cosmochimica Acta*, **68**, 3251–3260.

Luca, V. and Cardile, C.M. (1989) Improved detection of tetrahedral Fe^{3+} in nontronite SWa-1 by Mössbauer spectroscopy. *Clay Minerals*, **24**, 555–559.

Merola, R.B., Fournier, E.D., and McGuire, M.M. (2007) Spectroscopic investigations of Fe^{2+} complexation on nontronite clay. *Langmuir*, **23**, 1223–1226.

Neumann, A., Hofstetter, T.B., Luessi, M., Cirpka, O.A., Petit, S., and Schwarzenbach, R.P. (2008) Assessing the redox reactivity of structural iron in smectites using nitroaromatic compounds as kinetic probes. *Environmental Science & Technology*, **42,** 8381–8387.

Nzengung, V.A., Castillo, R.M., Gates, W.P., and Mills, G.L. (2001) Abiotic transformation of perchloroethylene in homogeneous dithionite solution and in suspensions of dithionite-treated clay minerals. *Environmental Science & Technology*, **35**, 2244–2251.

O'Reilly, S.E., Watkins, J., and Furukawa, Y. (2005) Secondary mineral formation associated with respiration of nontronite, NAu-1 by iron reducing bacteria. *Geochemical Transactions*, **6**, 67–76.

Ribeiro, F.R., Stucki, J.W., Larson, R.A., Marley, K.A., Komadel, P., and Fabris, J.D. (2004) Degradation of oxamyl by redox-modified smectites: Effects of pH, layer charge, and extent of Fe reduction. Pp. 471–474 in: *Applied Mineralogy, Developments in Science and Technology* (M. Pecchio *et al*., editors). ICAM, Sao Paulo, Brazil.

Rossman, G.R. (1988) Optical spectroscopy. Pp. 207–254 in: *Spectroscopic Methods in Mineralogy and Geology* (F.C. Hawthorne, editor). Mineralogical Society of America, Washington, D.C.

Scheinost, A.C., Chavernas, A., Barrón, V., and Torrent, J. (1998) Use and limitations of second-derivative diffuse reflectance spectroscopy in the visible to near-infrared range to identify and quantify Fe oxide minerals in soils. *Clays and Clay Minerals*, **46**, 528–536.

Schultz, C.A. and Grundl, T.J. (2000) pH dependence on reduction rate of 4-Cl-nitrobenzene by Fe(II)/montmorillonite systems. *Environmental Science & Technology*, **34**, 3641–3648.

Sherman, D.M. (1985) The electronic structures of Fe^{3+} coordination sites in iron oxides; applications to spectra, bonding, and magnetism. *Physics and Chemistry of Minerals*, **12**, 161–175.

Sherman, D.M. and Vergo, N. (1988) Optical (diffuse reflectance) and Mössbauer study of nontronite and related Fe-bearing smectites. *American Mineralogist*, **73**, 1346–1354.

Smith, G. and Strens, R.G.J. (1976) Intervalence-transfer absorption in some silicate, oxide and phosphate minerals. Pp. 583–612 in: *The Physics of Minerals and Rocks* (R.G.J. Strens, editor). Wiley, New York.

Sorensen, K.C., Stucki, J.W., Warner, R.E., and Plewa, M.J. (2004) Alteration of mammalian-cell toxicity of pesticides by structural iron(II) in ferruginous smectite. *Environmental Science & Technology*, **38**, 4383–4389.

Stucki, J.W., Lee, K., Zhang, L., and Larson, R.A. (2002) Effects of iron oxidation state on the surface and structural

properties of smectites. *Pure and Applied Chemistry*, **74**, 2145–2158.

Taran, M.N., Langer, K., and Platonov, A.N. (1996) Pressure- and temperature-effects on exchange-coupled-pair bands in electronic spectra of some oxygen-based iron-bearing minerals. *Physics and Chemistry of Minerals*, **23**, 230–236.

Tor, J.M., Xu, C.F., Stucki, J.W., Wander, M.M., and Sims, G.K. (2000) Trifluralin degradation under microbially induced nitrate and Fe(III) reducing conditions. *Environmental Science & Technology*, **34**, 3148–3152.

Vaniman, D. (2001) *Standard operating procedure for clay mineral and zeolite separation*. Los Alamos National Laboratory, NM, USA, SOP-09.05

Wu, J., Xia, Y., and Stucki, J.W. (2004) Color temperature indicator. US Patent No. 6,712,996.

Xu, J.C., Stucki, J.W., Wu, J., Kostka, J.E., and Sims, G.K. (2001) Fate of atrazine and alachlor in redox-treated ferruginous smectite. *Environmental Toxicology and Chemistry*, **20**, 2717–2724.

Yan, L.B. and Bailey, G.W. (2001) Sorption and abiotic redox transformation of nitrobenzene at the smectite-water interface. *Journal of Colloid and Interface Science*, **241**, 142–153.

Zhang, G., Dong, H., Kim, J., and Eberl, D.D. (2007) Microbial reduction of structural Fe^{3+} in nontronite by a thermophilic bacterium and its role in promoting the smectite to illite reaction. *American Mineralogist*, **92**, 1411–1419.

(*Received 13 January 2009; revised 30 July 2009; Ms. 272; A.E. S. Petit*)